nature geoscience

ARTICLES

https://doi.org/10.1038/s41561-020-0559-4

Early crust building enhanced on the Moon's nearside by mantle melting-point depression

Stephen M. Elardo[1,2,3]✉, Matthieu Laneuville[4], Francis M. McCubbin[5] and Charles K. Shearer[6]

The Moon's Earth-facing hemisphere hosts a geochemically anomalous region, the Procellarum KREEP Terrane, which is widely thought to have provided radiogenic heat for mantle melting from ~3.9 to ~1 billion years ago. However, there is no agreement on such a link between this region and the earliest pulse of post-differentiation crust-building magmatism on the Moon at ~4.37 billion years ago; whether this early magmatism was global or regional has been debated. Here we present results of high-temperature experiments that show the nearside geochemical anomaly may have caused asymmetric early crust building via mantle melting-point depression. Our results demonstrate that the anomalous enrichment in incompatible elements of this nearside reservoir dramatically lowers the melting temperature of the source rock for these magmas and may have resulted in 4 to 13 times more magma production under the nearside crust, even without any contribution from radioactivity. From thermal numerical modelling, we show that radiogenic heating compounds this effect and may have resulted in an asymmetric concentration of post-magma-ocean crust building on the lunar nearside. Our findings suggest that the nearside geochemical anomaly has influenced the thermal and magmatic evolution of the Moon over its entire post-differentiation history.

The differentiation of the terrestrial planets and large asteroids into cores, mantles and crusts is thought to have occurred throughout the inner solar system through extensive planetary melting (that is, magma oceans)[1]. Most magma-ocean models envision planets in this stage as homogeneous, well-mixed systems and do not, in their simple forms, predict lateral variations in composition and structure. However, fundamental asymmetries do occur in the inner solar system (for example, the Martian crustal dichotomy, tectonic plates on Earth), which can dramatically influence planetary geologic evolution. Although evidence for a global magma ocean on the Moon is arguably more robust than for any other planetary body, the Moon's crust also exhibits stark planet-scale asymmetries that are inconsistent with a homogeneously cooling body and are thought to have formed during magma-ocean differentiation[2–5]. The nearside and farside lunar crust is asymmetric in terms of (1) thickness[6,7], (2) the composition of the primary anorthosite derived from lunar magma ocean (LMO)[4] and (3) the distribution of both geochemically incompatible radioactive elements and erupted lavas[8–11].

The compositional asymmetry has been particularly influential on lunar evolution. A large terrane on the nearside hosts a geochemical reservoir, referred to by the acronym KREEP, which is highly enriched in its namesakes potassium (K), the rare earth elements (REEs), and phosphorus (P), in addition to the radioactive elements thorium (Th) and uranium (U), among other incompatible trace elements. Referred to as the Procellarum KREEP Terrane[8] (PKT), this region encompasses ~16% of the Moon's surface but hosts ~60% mare basaltic surface lava flows, and more broadly, ~97% of all mare basalts occur on the nearside[10]. These lavas are the product of the second major pulse of lunar magmatism and range in age from ~3.9 to ~1 billion years. Their spatial correlation with KREEP is probably no coincidence[9]. Thermal modelling of the interior strongly suggests that heat produced by the radioactive decay of K, Th and U provided a heat source for mantle melting under the nearside for billions of years and affected the Moon down to the core–mantle boundary, leaving a temperature anomaly in the mantle to the present day[12–14], demonstrating the importance of KREEP in influencing the Moon's long-term geologic evolution.

However, the Moon also experienced an earlier magmatic pulse beginning essentially immediately after LMO solidification at ~4.37 billion years ago (Ga) (refs. [15–18]) that resulted in an important crust-building event. These magmas, which crystallized into crustal rocks referred to as the Mg-suite due to their high Mg#s (the molar ratio of Mg/(Mg+Fe)), and later the alkali-suite (with relatively high abundances of alkalis), require planetary-scale mantle convection at the end of the LMO to form[19,20]. They have been proposed to arise either through decompression melting during mantle convection followed by assimilation of crustal anorthosite[21–23] or through melting of both anorthosite and mantle dunite at the crust–mantle interface[19,20,24]. The role of KREEP, or lack thereof, in the origin of this crust-building event is highly debated, as is the spatial and volumetric extent of Mg-suite magmatism. Samples of the Mg-suite collected by five of the six landed Apollo missions, whose landing sites were all within or adjacent to the PKT, demonstrate the rocks are KREEP-rich and widely distributed across the nearside[19,24,25], leading to the suggestion that the asymmetric distribution of KREEP on the nearside and the heat it produced initiated Mg-suite magmatism and that this crust-building event was regional rather than global[13,26]. This view has been challenged both by laboratory experiments and spectroscopic remote observations of the global crust, which may indicate outcrops of Mg-suite rocks across the Moon[27–31], and by observations of new samples in lunar meteorites that may point to Mg-suite rocks without a link to KREEP[32]. Neither interpretation is definitive, yet the resolution to this debate will reveal the extent of early crust building and the degree to which planetary-scale asymmetries have dictated the thermal and magmatic evolution of the Moon.

[1]Department of Geological Sciences, University of Florida, Gainesville, FL, USA. [2]Geophysical Laboratory, Carnegie Institution for Science, Washington, DC, USA. [3]Department of Physics, Astronomy, and Geosciences, Towson University, Towson, MD, USA. [4]Earth-Life Science Institute, Tokyo Institute of Technology, Tokyo, Japan. [5]NASA Johnson Space Center, Houston, TX, USA. [6]Institute of Meteoritics, University of New Mexico, Albuquerque, NM, USA. ✉e-mail: selardo@ufl.edu

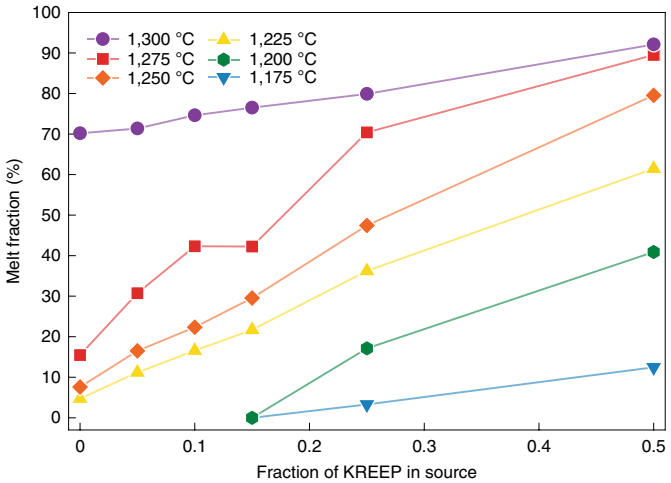

Fig. 1 | The effects of KREEP on melt production in Mg-suite sources. The results of high-temperature experiments show that the addition of KREEP to an analogue Mg-suite source rock, consisting of dunite and anorthosite, dramatically lowers its melting temperature. Each line is an isotherm showing the amount of melt present at a given temperature as a function of the fraction of KREEP by weight in the dunite–anorthosite starting mixture.

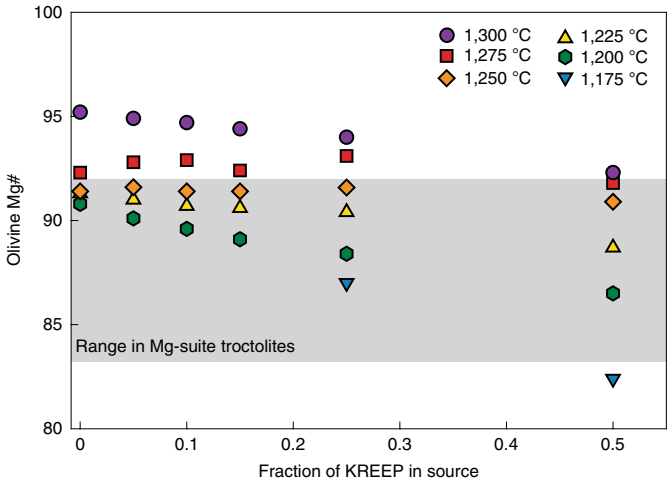

Fig. 2 | The composition of experimental olivine compared with Apollo Mg-suite samples. The composition of equilibrium olivine produced in our experiments as a function of the fraction of KREEP by weight in the dunite–anorthosite starting mixture. The grey band denotes the range of olivine compositions found in Mg-suite troctolites and spinel troctolites in the Apollo sample collection. The broad agreement between experimentally produced olivine and olivine found in natural samples demonstrates that our experimental melt compositions are consistent with Mg-suite parental melts.

Crust building via melting-point depression

The power of KREEP in producing mantle partial melts has previously thought to lie in radiogenic heat production, and with Th and U abundances over 700 times those in primitive chondrite meteorites[33], heat production was undoubtedly a driving force for melting[12–14]. However, a key component of the ability of KREEP to aid in melt production is melting-point depression. This effect has thus far been unexplored. The KREEP reservoir formed as the last remaining magmatic liquid in the LMO after extensive fractional crystallization formed the underlying mantle and overlying crust, and therefore, by definition, KREEP has a much lower melting point (that is, solidus) than both. When high-Mg# dunites from the deep mantle, with a very high melting temperature, reach the base of the anorthosite crust as a result of density-driven mantle convection[20,34–36], KREEP has the potential to induce melting of the three-component system due to the change in bulk chemical composition caused by the addition of KREEP. To determine the magnitude of this effect, we conducted a series of high-temperature melting experiments on a 50/50 mixture of natural olivine and anorthite from San Carlos, AZ, and the Miyake-jima volcano, Japan, respectively. San Carlos olivine (SCO, Mg# 90) and Miyake-jima anorthite (MJA, An# 96, where An# is the molar ratio of Ca/(Ca+Na+K)) have compositions that make them excellent analogues for the mantle dunites[20] and the anorthosite crust[37]. This mixture was then split and combined with 5%, 10%, 15%, 25% or 50% of a synthetic KREEP composition[33]. The baseline KREEP-free olivine–anorthite mixture represents an analogue for the crust–mantle interface on the Moon's farside and offers a point of comparison with the KREEP-bearing mixtures. These experiments were conducted at 1 atm at lunar-like redox conditions and temperatures between 1,300 °C and 1,175 °C for 4–8 d to ensure equilibrium was closely approached.

The results of our experiments show that the potential for KREEP to produce Mg-suite magmas though melting-point depression is dramatic. At a given temperature, the presence of up to 50% KREEP in the olivine–anorthite mixture results in between 2 and 13 times more melt than in the experiments without KREEP (Fig. 1 and Supplementary Information). At 1,250 °C, for example, the KREEP-free system produces an 8% partial melt, yet with 50% KREEP, the melt fraction reaches 79%. However, the ability of KREEP to produce more magma in our nearside-analogous experiments is irrelevant if the compositions of those melts do not match the compositions of the natural magmas that crystallized into the Mg-suite rocks. We assessed this constraint by comparing the Mg#'s of olivine from our experiments with the Mg#'s of primitive (that is, the first to form from a magma) Mg-suite troctolite samples collected by the Apollo missions (Fig. 2), and the calculated REE patterns of our experimental melts with the estimated REE abundances in troctolite parental magmas[17,25] (Fig. 3). Troctolites, which are cumulate rocks consisting dominantly of olivine and plagioclase, represent the most primitive Mg-suite rocks, meaning they offer the best point of comparison to assess whether our experimental melt compositions match the natural magmas (see Supplementary Information). With only one exception at 15% KREEP, only mantle source region compositions with 25–50% KREEP produce partial melts that match both the Mg# and REE abundances of Mg-suite troctolites and their parental magmas (Figs. 2 and 3). These model source regions produce 4–13 times as much melt as KREEP-free sources and over degrees of partial melting ranging from 3% to 79%. At temperatures that produce these melts (1,175–1,250 °C), KREEP-free source regions produce 0–8% partial melt. These results strongly suggest that KREEP-induced melting-point depression probably resulted in dramatically more crust-building magma under the Moon's nearside relative to the farside.

Contributions from radiogenic heat production

The results of our experiments demonstrate the propensity of KREEP to lower the melting temperature of the mantle source regions of Mg-suite magmas. However, the heat produced from the radioactive decay of K, Th and U will also contribute to melting. To estimate the magnitude of the contribution from radiogenic heat, we conducted thermal evolution calculations on model Mg-suite source regions. There are many uncertainties in calculating absolute temperatures, including the initial mantle temperature profile, cooling rate at the crust–mantle interface at ~4.37 Ga, the exact composition and KREEP content of Mg-suite magma source regions and time between formation of the KREEP reservoir and the onset of Mg-suite magma melting. Therefore, we have taken the approach of calculating the change in temperature (ΔT) of a series of dunite–anorthosite

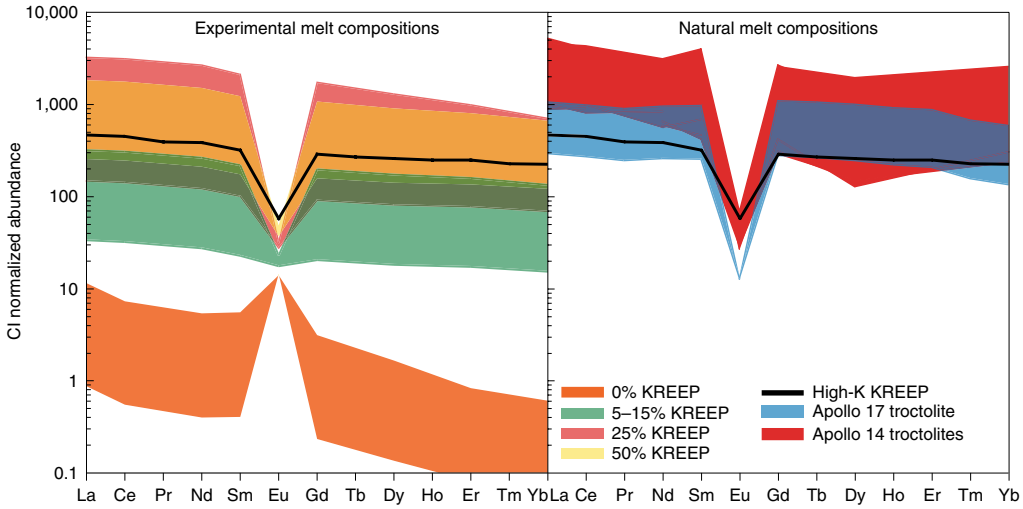

Fig. 3 | Calculated REE abundances in experimental melts compared with Mg-suite parental melts. The calculated chondrite-normalized abundances of REEs in our experimental melts (left panel) compared with the abundances of REEs in Mg-suite troctolite parental magmas (right panel; see Supplementary Information for calculation methods) demonstrate that our model produces melts that match the compositions of Mg-suite magmas. The magnitude of REE enrichment in the melt depends on both the REE abundances in the mantle source and the degree of partial melting. The composition of pure high-K KREEP[33] is shown in both panels for comparison.

source regions with 0–50% KREEP for a given cooling rate. These calculations considered the range of post-LMO lower crustal cooling rates from the asymmetric lunar thermal evolution models of Laneuville et al.[12,38] (0.2–2.5 K Myr^{-1}, or roughly 1–10^{-10} W kg^{-1}).

Our results show that, irrespective of cooling rate considered, Mg-suite source regions heat up by tens of K Myr^{-1} when they contain at least 25% KREEP ($f > 0.25$) and have positive ΔT even at KREEP contents of less than 5% at the lowest possible cooling rates (Fig. 4). Conversely, Mg-suite sources cool down at almost all cooling rates for KREEP contents of <~5%. These results, combined with trace element analyses that show Mg-suite magmas were KREEP-rich[25,39,40] (Fig. 3), demonstrate that radioactivity resulted in an increase in the temperature of Mg-suite mantle sources (Fig. 4) and the production of crust-building magmas under the nearside, but probably not under the farside. It should be noted that these estimates are valid only for KREEP fractions close to what was used by Laneuville et al.[38], which corresponds to about $f < 0.3$. Outside of that range, the cooling rate will be affected by the strong increase in temperature. For example, at $\Delta T = 50$ K Myr^{-1}, a source region would be heated by 3,000 K over 60 Myr (that is, from 4.43 to 4.37 Ga), which is the maximum possible time between KREEP formation and the onset of Mg-suite magmatism derived from Apollo sample geochronology[15,18,41] if no change occurred in cooling rate, which is clearly unrealistic. However, these results, combined with those of our experiments, demonstrate the positive feedback that KREEP had on mantle melting: the more KREEP in a mantle source, the lower the melting temperature, the higher the radiogenic heat production and the more magma that was produced.

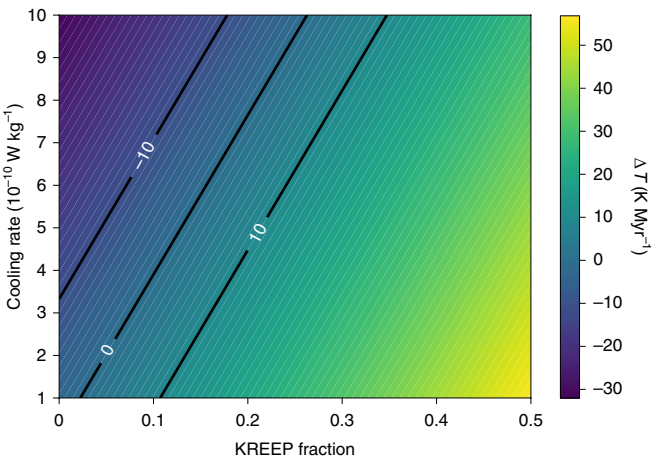

Fig. 4 | The ΔT of Mg-suite source regions due to radiogenic heating. The results of thermal evolution calculations show the ΔT of the dunite–anorthosite source regions of Mg-suite parental magmas with KREEP contents up to 50% by weight and how the ΔT varies over the range in possible cooling rates (in 10^{-10} W kg^{-1}) at the lunar crust–mantle interface at ~4.4 Ga (ref. [38]). The ΔT increases with increasing KREEP content due to the radiogenic heat produced by decay of K, Th and U. Black lines denote the parameter space where radiogenic heating is perfectly balanced by the cooling rate ('0' line) and where the T increases or decreases by 10 K Myr^{-1} ('10' and '−10' lines).

Regional rather than global early lunar crust building

Our results challenge the notion that crust-building magmatism that immediately followed the LMO was a Moon-wide event. The combination of radiogenic heat production and the ability of KREEP to lower the melting point of Mg-suite source rocks, as demonstrated here, would have led to considerably more crust-building magmatism under the nearside relative to the farside. Our findings do not preclude the possibility of occurrences of some Mg-suite rocks throughout the lunar crust. Decompression melting of lunar mantle dunites followed by assimilation of crustal anorthosite has been proposed as a mechanism for generating Mg-suite magmas Moon-wide[21,22,28]. However, this model faces notable challenges. Dunites in the lunar mantle are thought to have been very poor in aluminium[20,42,43], meaning they had a very high melting temperature. This necessitates anorthosite assimilation to reach plagioclase saturation, a process that faces substantial limitations from an energy budget standpoint[21,44]. Calculations of fractional melting using the pMELTS algorithm[45–47] show that deep-mantle dunites produce only ~3–10% melt during adiabatic decompression, depending on the initial mantle temperature and amount of trapped LMO liquid (see Supplementary Information). Furthermore, recent geodynamic

modelling suggested that convective overturn in the mantle, which brings these dunites from the lower mantle to the base of the crust, may begin before the end of magma-ocean crystallization[36,48,49], in which case any magmas formed through decompression melting would not have been able to move past the residual LMO to reach the crust.

Our results show that the hemispheric compositional asymmetries on the Moon began to have a dramatic effect on magma production immediately after lunar differentiation. The large concentration of heat-producing elements on the Moon's nearside not only had the potential to act as a heat source for melting but also lowered melting temperatures at the crust–mantle interface in a way that could have produced ~4–13 times more crust-building magmas than would have occurred on the farside. The positive feedback among the amount of KREEP in a source region, KREEP's ability to depress melting temperatures and its penchant for heat production probably resulted in asymmetric crust building on the Moon's nearside and demonstrates the important role that KREEP and its concentration on the nearside played in the thermal and magmatic evolution of the Moon throughout its entire ~4.4 Gyr history.

Online content

Any methods, additional references, Nature Research reporting summaries, source data, extended data, supplementary information, acknowledgements, peer review information; details of author contributions and competing interests; and statements of data and code availability are available at https://doi.org/10.1038/s41561-020-0559-4.

Received: 1 October 2019; Accepted: 20 February 2020;
Published online: 30 March 2020

References

1. Elkins-Tanton, L. T. Magma oceans in the inner Solar System. *Annu. Rev. Earth Planet. Sci.* **40**, 113–139 (2012).
2. Wasson, J. T. & Warren, P. H. Contribution of the mantle to the lunar asymmetry. *Icarus* **44**, 752–771 (1980).
3. Loper, D. E. & Werner, C. L. On lunar asymmetries 1. Tilted convection and crustal asymmetry. *J. Geophys. Res. Planets* **107**, 5046 (2002).
4. Ohtake, M. et al. Asymmetric crustal growth on the Moon indicated by primitive farside highland materials. *Nat. Geosci.* **5**, 384–388 (2012).
5. Quillen, A. C., Martini, L. & Nakajima, M. Near/far side asymmetry in the tidally heated Moon. *Icarus* **329**, 182–196 (2019).
6. Wieczorek, M. A. et al. The crust of the Moon as seen by GRAIL. *Science* **339**, 671–675 (2013).
7. Zuber, M. T., Smith, D. E., Lemoine, F. G. & Neumann, G. A. The shape and internal structure of the Moon from the Clementine mission. *Science* **266**, 1839–1843 (1994).
8. Jolliff, B. L., Gillis, J. J., Haskin, L. A., Korotev, R. L. & Wieczorek, M. A. Major lunar crustal terranes: surface expressions and crust–mantle origins. *J. Geophys. Res.* **105**, 4197–4216 (2000).
9. Lawrence, D. J. et al. Global elemental maps of the Moon: the Lunar Prospector gamma-ray spectrometer. *Science* **281**, 1484–1489 (1998).
10. Head, J. W. Lunar volcanism in space and time. *Rev. Geophys.* **14**, 265–300 (1976).
11. Metzger, A., Haines, E., Parker, R. & Radocinski, R. Thorium concentrations in the lunar surface I: regional values and crustal content. In *Proc. 8th Lunar Science Conference* 949–999 (Pergamon, 1977).
12. Laneuville, M., Wieczorek, M. A., Breuer, D. & Tosi, N. Asymmetric thermal evolution of the Moon. *J. Geophys. Res. Planets* **118**, 1435–1452 (2013).
13. Wieczorek, M. A. & Phillips, R. J. The "Procellarum KREEP Terrane": implications for mare volcanism and lunar evolution. *J. Geophys. Res. Planets* **105**, 20417–20430 (2000).
14. Hess, P. C. & Parmentier, E. M. Thermal evolution of a thicker KREEP liquid layer. *J. Geophys. Res. Planets* **106**, 28023–28032 (2001).
15. Borg, L. E., Gaffney, A. M. & Shearer, C. K. A review of lunar chronology revealing a preponderance of 4.34–4.37 Ga ages. *Meteorit. Planet. Sci.* **50**, 715–732 (2015).
16. Carlson, R. W., Borg, L. E., Gaffney, A. M. & Boyet, M. Rb–Sr, Sm–Nd and Lu–Hf isotope systematics of the lunar Mg-suite: the age of the lunar crust and its relation to the time of Moon formation. *Philos. Trans. R. Soc. A* **372**, 20130246 (2014).
17. Borg, L. E., Connelly, J. N., Cassata, W. S., Gaffney, A. M. & Bizzarro, M. Chronologic implications for slow cooling of troctolite 76535 and temporal relationships between the Mg-suite and the ferroan anorthosite suite. *Geochim. Cosmochim. Acta* **201**, 377–391 (2017).
18. Gaffney, A. M. & Borg, L. E. A young solidification age for the lunar magma ocean. *Geochim. Cosmochim. Acta* **140**, 227–240 (2014).
19. Shearer, C. K., Elardo, S. M., Petro, N. E., Borg, L. E. & McCubbin, F. M. Origin of the lunar highlands Mg-suite: an integrated petrology, geochemistry, chronology, and remote sensing perspective. *Am. Mineral.* **100**, 294–325 (2015).
20. Elardo, S. M., Draper, D. S. & Shearer, C. K. Lunar magma ocean crystallization revisited: bulk composition, early cumulate mineralogy, and the source regions of the highlands Mg-suite. *Geochim. Cosmochim. Acta* **75**, 3024–3045 (2011).
21. Hess, P. C. Petrogenesis of lunar troctolites. *J. Geophys. Res. Planets* **99**, 19083–19093 (1994).
22. Prissel, T. C., Parman, S. W. & Head, J. W. Formation of the lunar highlands Mg-suite as told by spinel. *Am. Mineral.* **101**, 1624–1635 (2016).
23. Warren, P. H. The origin of pristine KREEP: effects of mixing between urKREEP and the magmas parental to the Mg-rich cumulates. In *Proc. 18th Lunar and Planetary Science Conference* 233–241 (Cambridge Univ. Press/ Lunar and Planetary Institute, 1988).
24. Shearer, C. K. & Papike, J. J. Early crustal building processes on the Moon: models for the petrogenesis of the magnesian suite. *Geochim. Cosmochim. Acta* **69**, 3445–3461 (2005).
25. Shervais, J. W. & McGee, J. J. Ion and electron microprobe study of troctolites, norite, and anorthosites from Apollo 14: evidence for urKREEP assimilation during petrogenesis of Apollo 14 Mg-suite rocks. *Geochim. Cosmochim. Acta* **62**, 3009–3023 (1998).
26. Korotev, R. L. The great lunar hot spot and the composition and origin of the Apollo mafic ("LKFM") impact-melt breccias. *J. Geophys. Res. Planets* **105**, 4317–4345 (2000).
27. Pieters, C. M. et al. The distribution of Mg-spinel across the Moon and constraints on crustal origin. *Am. Mineral.* **99**, 1893–1910 (2014).
28. Prissel, T. C. et al. Pink Moon: the petrogenesis of pink spinel anorthosites and implications concerning Mg-suite magmatism. *Earth Planet. Sci. Lett.* **403**, 144–156 (2014).
29. Dhingra, D. et al. Compositional diversity at Theophilus Crater: understanding the geological context of Mg-spinel bearing central peaks. *Geophys. Res. Lett.* **38**, L11201 (2011).
30. Jackson, C. R. et al. Visible-infrared spectral properties of iron-bearing aluminate spinel under lunar-like redox conditions. *Am. Mineral.* **99**, 1821–1833 (2014).
31. Williams, K. B. et al. Reflectance spectroscopy of chromium-bearing spinel with application to recent orbital data from the Moon. *Am. Mineral.* **101**, 726–734 (2016).
32. Treiman, A. H. & Gross, J. A rock fragment related to the magnesian suite in lunar meteorite Allan Hills (ALHA) 81005. *Am. Mineral.* **100**, 414–426 (2015).
33. Warren, P. H. in *Workshop on Moon in Transition: Apollo 14, KREEP, and Evolved Lunar Rocks* Technical Report No. 89-03 (eds Taylor, G. J. & Warren, P. H.) 149–153 (LPI, 1989).
34. Hess, P. C. & Parmentier, E. M. A model for the thermal and chemical evolution of the Moon's interior: implications for the onset of mare volcanism. *Earth Planet. Sci. Lett.* **134**, 501–514 (1995).
35. Elkins Tanton, L. T., Van Orman, J. A., Hager, B. H. & Grove, T. L. Re-examination of the lunar magma ocean cumulate overturn hypothesis: melting or mixing is required. *Earth Planet. Sci. Lett.* **196**, 239–249 (2002).
36. Boukaré, C.-E., Parmentier, E. & Parman, S. Timing of mantle overturn during magma ocean solidification. *Earth Planet. Sci. Lett.* **491**, 216–225 (2018).
37. Nakamura, N., Masuda, A., Tanaka, T. & Kurasawa, H. Chemical compositions and rare-earth features of four Apollo 16 samples. In *Proc. 4th Lunar Science Conference* Vol. 2, 1407–1414 (Pergamon, 1973).
38. Laneuville, M., Taylor, J. & Wieczorek, M. A. Distribution of radioactive heat sources and thermal history of the Moon. *J. Geophys. Res. Planets* **123**, 3144–3166 (2018).
39. Papike, J. J., Fowler, G. W., Shearer, C. K. & Layne, G. D. Ion microprobe investigation of plagioclase and orthopyroxene from lunar Mg-suite norites: implications for calculating parental melt REE concentrations and for assessing postcrystallization REE redistribution. *Geochim. Cosmochim. Acta* **60**, 3967–3978 (1996).
40. Papike, J. J., Fowler, G. W. & Shearer, C. K. Orthopyroxene as a recorder of lunar crust evolution: an ion microprobe investigation of Mg-suite norites. *Am. Mineral.* **79**, 796–800 (1994).
41. Connelly, J. N. & Bizzarro, M. Lead isotope evidence for a young formation age of the Earth–Moon system. *Earth Planet. Sci. Lett.* **452**, 36–43 (2016).
42. Charlier, B., Grove, T. L., Namur, O. & Holtz, F. Crystallization of the lunar magma ocean and the primordial mantle–crust differentiation of the Moon. *Geochim. Cosmochim. Acta* **234**, 50–69 (2018).

43. Rapp, J. F. & Draper, D. S. Fractional crystallization of the lunar magma ocean: updating the dominant paradigm. *Meteorit. Planet. Sci.* **53**, 1432–1455 (2018).
44. Treiman, A. H., Kulis, M. E. J. & Glazner, A. F. Spinel-anorthosites on the Moon: impact melt origins suggested by enthalpy constraints. *Am. Mineral.* **104**, 370–384 (2019).
45. Smith, P. M. & Asimow, P. D. Adiabat_1ph: a new public front-end to the MELTS, pMELTS, and pHMELTS models. *Geochem. Geophys. Geosyst.* **6**, Q02004 (2005).
46. Asimow, P. D. & Ghiorso, M. S. Algorithmic modifications extending MELTS to calculate subsolidus phase relations. *Am. Mineral.* **83**, 1127–1132 (1998).
47. Ghiorso, M. S., Hirschmann, M. M., Reiners, P. W. & Kress, V. C. The pMELTS: a revision of MELTS for improved calculation of phase relations and major element partitioning related to partial melting of the mantle to 3 GPa. *Geochem. Geophys. Geosyst.* **3**, https://doi.org/10.1029/2001GC000217 (2002).
48. Elkins-Tanton, L. T., Burgess, S. & Yin, Q. Z. The lunar magma ocean: reconciling the solidification process with lunar petrology and geochronology. *Earth Planet. Sci. Lett.* **304**, 326–336 (2011).
49. Morison, A., Labrosse, S., Deguen, R. & Alboussiere, T. Timescale of overturn in a magma ocean cumulate. *Earth Planet. Sci. Lett.* **516**, 25–36 (2019).

Methods

Experimental starting materials. The base KREEP-free olivine–anorthite mixture that simulated Mg-suite magma source rock (Supplementary Table 1) was made from natural SCO (Mg# 90) and MJA (An# 96). Crystals of SCO were cleaned with multiple successive ultrasonic baths in ethanol followed by soaking in warm 6 N HCl to remove desert contamination before being crushed with an agate mortar and pestle. Visible pyroxene and oxide impurities, and any substantially weathered or oxidized fragments, were removed before the sample was ground into a fine powder under ethanol. A powdered sample of MJA that was previously purified with a Frantz magnetic separator was provided by K. Donaldson Hanna. The powdered SCO and MJA were then combined in a proportion of 50/50 by weight and ground under ethanol until homogeneous (Supplementary Table 2).

A synthetic mixture with the composition of high-K KREEP defined by Warren[33] was made using reagent-grade oxides and carbonates. The mixture, consisting of all major and minor elements in high-K KREEP, was combined in a stepwise fashion and ground under ethanol until homogeneous. Subsequently, all REEs and other trace elements with abundances in high-K KREEP of 200 ppm or greater were added to the mixture using Specpure plasma standard solutions in 2% HNO_3. The nitric acid was allowed to evaporate in a fume hood. The synthetic KREEP mixture was then combined with aliquots of the 50/50 SCO–MJA mixture to create five additional experimental starting materials with 5%, 10%, 15%, 25% and 50% KREEP by weight (Supplementary Table 2). The mixtures were ground under ethanol until homogeneous.

High-temperature experiments. High-temperature phase equilibrium experiments at ambient pressure were conducted in a Deltech vertical gas-mixing furnace at the Geophysical Laboratory, Carnegie Institution for Science. Starting materials were mixed with a 3% polyvinyl alcohol solution to form a paste and suspended from a thin-gauge Re-wire loop in the hotspot of the Deltech furnace. Experiments were held above the liquidus at 1,500 °C at a log fO_2 corresponding to the iron-wüstite buffer[50] using mixtures of CO and CO_2 for ~2 h before being quenched into distilled water, forming a glass. Glasses were left attached to the Re loops and then reintroduced into the furnace, two compositions at a time, at each temperature of interest. The fO_2 was maintained at iron-wüstite for the duration of the experiments using total gas flow rates of ~0.5 $cm^3 s^{-1}$. Redox conditions within the furnace were assessed with a Y_2O_3-stabilized ZrO_2 electrode using air as a reference gas. The estimated error on this measurement is ≤0.2 log units. The electromotive force (emf) of the experimental gas mixture was measured before each experiment and was confirmed after selected experiments. The emf was found to vary by <5 mV. Temperature was monitored using a type S ($Pt_{10}Rh$/Pt) thermocouple and controlled using a Eurotherm controller. Experimental durations were between ~4 and 8 d depending on temperature and experiments were quenched into water. The long durations of the experiments ensured a close approach to equilibrium was achieved.

Although these experiments were meant to investigate melting conditions at the lunar crust–mantle interface, which resides at a pressure of ~0.2 GPa (ref. [48]), ambient-pressure controlled-atmosphere experiments were selected here over elevated-pressure experiments for a number of reasons. First, at ambient pressure, the solubility of water in silicate melts is negligible[51], which is advantageous because water is known to dramatically lower the solidus temperature of silicate systems at elevated pressure[52,53]. Water contents of high-pressure experiments are also variable and difficult to precisely control. Although water in lunar materials has been the focus of extensive study over the past decade, the lunar mantle is thought to contain much less water[54] than is typically present in high-pressure experiments. Second, the Deltech furnace allows for very precise control of fO_2 conditions with the use of mixed gases, whereas fO_2 is more difficult to precisely control at elevated pressure. Last, the difference in phase relations in lunar-analogous systems between ambient pressure and 0.2 GPa is negligible[55] and thus has little effect on our results.

Ambient-pressure experiments, however, often result in the loss of volatile species (for example, Na, K, S), and this was the case for the experiments presented here. Loss of Na and K resulted in plagioclase in our experiments having the composition of nearly pure endmember anorthite. Experiments on compositions with higher amounts of KREEP experienced more-volatile loss due to the higher abundances of Na and K in KREEP versus the base SCO–MJA mix. However, this does not affect the conclusions of this work. Retention of volatile species (or the presence of water concentrated in KREEP) would have resulted in lower solidus temperatures for more KREEP-rich compositions and thus would have further enhanced the solidus-depressing effects of KREEP, strengthening our conclusions. Therefore, the effect of KREEP on lowering the solidus temperature demonstrated here is a lower limit.

Electron microprobe analyses. Experimental run products were mounted in epoxy, ground and polished flat to expose a cross-section roughly through the middle of each experimental run product before carbon coating. Mineral and quenched melt phases were analysed for major and most minor elements using the JEOL JXA-8530F field emission electron microprobe at the Geophysical Laboratory. Operating conditions were 15 kV, 20 nA and spot sizes between 1 and 10 µm. Spot sizes on the high end of that range, especially for quenched melt and plagioclase, were used whenever textures permitted. Standards were diopside, Na-bearing diopside (DJ-35), pyrope, orthoclase, chromite, ilmenite, spessartine, Durango apatite, zircon, wollastonite and Springwater olivine. The quality of analyses was assessed on the basis of stoichiometric constraints. Experimental results can be found in Supplementary Tables 3 and 4.

Thermal evolution calculations. We computed the change in temperature of a hypothetical Mg-suite mantle source rock consisting of a 50/50 dunite and ferroan anorthosite (FAN) mixture with variable amounts of KREEP (Supplementary Table 5) as a function of KREEP content from 0% to 50%. For a given concentration of Th, U and K, we computed the heating rate[56] as:

$$H = 0.9928C_0^{\mathrm{U}}H^{\mathrm{U}^{238}}\exp\left(\frac{t\ln 2}{\tau_{1/2}^{\mathrm{U}^{238}}}\right) + 0.0071C_0^{\mathrm{U}}H^{\mathrm{U}^{235}}\exp\left(\frac{t\ln 2}{\tau_{1/2}^{\mathrm{U}^{235}}}\right) + C_0^{\mathrm{Th}}H^{\mathrm{Th}^{232}}\exp\left(\frac{t\ln 2}{\tau_{1/2}^{\mathrm{Th}^{232}}}\right) + 1.19\times 10^{-4}C_0^{\mathrm{K}}H^{\mathrm{K}^{40}}\exp\left(\frac{t\ln 2}{\tau_{1/2}^{\mathrm{K}^{40}}}\right)$$

where C_0 is the initial concentration of each isotope in the mantle source, H is the specific heat production rate for each isotope, t is time and $\tau_{1/2}$ is the isotope-specific half-life (Supplementary Table 5). We consider the range of lower crustal cooling rate Q from Laneuville et al.[38] over the 4.43 to 4.37 Ga time frame, which is between 0.2 and 2.5 K Myr^{-1} at the bottom of the crust. For a given model, the cooling rate variation over the 4.43 to 4.37 Ga interval is negligible, so we use the 4.4 Ga value for this calculation.

We compared the heating rate due to the inclusion of KREEP with fraction f with the range of cooling rates to the crust (Fig. 3). Specifically, we calculated $\Delta T = (H(f) - Q)/c_p$, where c_p is the specific heat of mantle material (1,000 J kg^{-1} K^{-1}) and H and Q are in W kg^{-1}. These estimates do not take melting itself into account as the point was to assess the relative impact of radioactive heating compared with melting-point depression. Source regions would not heat endlessly beyond melting as Th, U and K are incompatible elements, which would be extracted from Mg-suite source regions via the melting process.

Data availability

The data supporting the findings of this study are available within the article and its Supplementary Information files.

Code availability

The code used for the thermal evolution calculations presented here is available from M.L. upon request. Email: mlaneuville@elsi.jp.

References

50. O'Neill, H. S. C. & Pownceby, M. I. Thermodynamic data from redox reactions at high-temperatures 1: an experimental and theoretical assessment of the electrochemical ethod using stabilized zirconia electrolytes, with revised values for the Fe–FeO, Co–CoO, Ni–NiO and Cu–Cu_2O oxygen buffers, and new data for the W–WO_2 buffer. *Contrib. Mineral. Petrol.* **114**, 296–314 (1993).
51. Dixon, J. E. & Stolper, E. M. An experimental study of water and carbon dioxide solubilities in mid-ocean ridge basaltic liquids: part II, applications to degassing. *J. Petrol.* **36**, 1633–1646 (1995).
52. Yoder, H. Jr Diopside–anorthite–water at five and ten kilobars and its bearing on explosive volcanism. *Year B Carnegie Inst. Wash.* **64**, 82–89 (1965).
53. Kushiro, I. The system forsterite–diopside–silica with and without water at high pressures. *Am. J. Sci.* **267**, 269–294 (1969).
54. McCubbin, F. M. et al. Magmatic volatiles (H, C, N, F, S, Cl) in the lunar mantle, crust, and regolith: abundances, distributions, processes, and reservoirs. *Am. Mineral.* **100**, 1668–1707 (2015).
55. Merrill, R. B. & Williams, R. J. The system anorthite–forsterite–fayalite–silica to 2 kbar with lunar petrologic applications. In *Proc. 6th Lunar Science Conference* 959–971 (Pergamon Press, 1975).
56. Breuer, D. in *Solar System* (ed. Trümper, J. E.) 323–344 (Springer, 2009).

Acknowledgements

We are grateful to A. Shahar (Carnegie) and the Carnegie Institution for Science for access to the experimental facilities there, E. Bullock (Carnegie) for assistance with EMP analyses and K. Donaldson Hanna (UCF) for kindly providing us an aliquot of Miyake-jima anorthite. This work was funded by a NASA Solar System Workings grant (NNX16AQ17G/80NSSC19K0752) to S.M.E.

Author contributions

S.M.E., F.M.M. and C.K.S. developed the concept of this study. S.M.E. conducted all experiments and analyses. M.L. conducted all heat production calculations. All authors contributed to data interpretation and preparation of the manuscript.

Competing interests

The authors declare no competing interests.

Additional information

Supplementary information is available for this paper at https://doi.org/10.1038/s41561-020-0559-4.

Correspondence and requests for materials should be addressed to S.M.E.

Peer review information Primary Handling Editor: Stefan Lachowycz.